Heliyon 11 (2025) e41628

Contents lists available at ScienceDirect

Heliyon

journal homepage: www.cell.com/heliyon

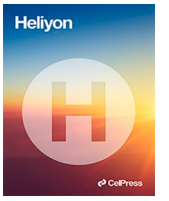

Research article

PPARG/SPP1/CD44 signaling pathway in alveolar macrophages: Mechanisms of lipid dysregulation and therapeutic targets in idiopathic pulmonary fibrosis

Ganggang Li [a], Yuwei Zhang [a], Huanyu Jiang [d], Xuanyu Wu [a], Yanwei Hao [a], Yuchen Su [a], Yutong Zou [a], Wenjia Xian [a], Fei Wang [a,**], Quanyu Du [b,c,*]

[a] Department of Geriatrics, Hospital of Chengdu University of Traditional Chinese Medicine, Chengdu, Sichuan, 610072, China
[b] Department of Endocrinology, Hospital of Chengdu University of Traditional Chinese Medicine, Chengdu, Sichuan, 610072, China
[c] TCM Regulating Metabolic Diseases Key Laboratory of Sichuan Province, Chengdu, Sichuan, 610072, China
[d] School of Basic Medical Sciences, Chengdu University of Traditional Chinese Medicine, Chengdu, Sichuan, 611130, China

ARTICLE INFO

Keywords:
Idiopathic pulmonary fibrosis
Lipid metabolism
Alveolar macrophage
PPARG
SPP1
CD44

ABSTRACT

Idiopathic pulmonary fibrosis (IPF) is a chronic and progressive interstitial lung disease. It is characterized by inflammation and fibrosis in the lung parenchyma and interstitium. Given its poor prognosis and limited treatment options, understanding the underlying molecular mechanisms is crucial. Recent evidence suggests that lipid metabolism plays a pivotal role in IPF pathogenesis, however, the precise mechanisms remain poorly understood. To address this, we analyzed 12 bulk RNA-seq and 2 single-cell RNA-seq datasets from the GEO database using machine learning approaches. As a result, we identified four key lipid-related genes—PPARG, SPP1, CASP3, and PECAM1—that are expressed across various cell types. Specifically, in alveolar macrophages (AMs), we observed that PPARG was significantly downregulated, while SPP1 was highly expressed. Importantly, PPARG serves as a transcriptional regulator of SPP1, which in turn mediates intercellular signaling via CD44. Based on these findings, we propose a novel PPARG/SPP1/CD44 signaling pathway in AMs, which modulates lipid metabolism and likely contributes to the progression of fibrosis in IPF. Moreover, network pharmacology analysis identified several herbal compounds that target PPARG, offering potential therapeutic opportunities. In conclusion, these findings highlight the critical role of lipid metabolism in IPF and present novel molecular targets for the development of future therapeutic strategies.

1. Introduction

Idiopathic pulmonary fibrosis (IPF) is a progressive and fatal lung disease with a median survival of only 3–5 years after diagnosis [1–5]. Despite the approval of antifibrotic drugs such as nintedanib and pirfenidone, these treatments merely alleviate symptoms and slow disease progression, with lung transplantation being the only definitive intervention to reverse fibrosis [6–8]. The intricate pathogenesis of IPF, driven by diverse cellular and molecular mechanisms, complicates the development of effective therapies. Recent

* Corresponding author. Department of Endocrinology, Hospital of Chengdu University of Traditional Chinese Medicine, Chengdu, Sichuan, 610072, China.
** Corresponding author.
E-mail addresses: wangfei@cdutcm.edu.cn (F. Wang), quanydu@cdutcm.edu.cn (Q. Du).

https://doi.org/10.1016/j.heliyon.2025.e41628
Received 8 August 2024; Received in revised form 30 December 2024; Accepted 1 January 2025
Available online 2 January 2025

studies have highlighted the potential of traditional Chinese herbal medicines to target key signaling pathways involved in fibrosis, offering novel therapeutic avenues for IPF treatment [9,10].

Lipids, critical cellular components, are involved in energy storage, membrane structure, and signaling [11–13]. Their role in lung diseases such as lung cancer, COPD, and asthma is well documented [14–17]. Recent research suggests that lipid metabolism may also be a key factor in IPF, though the specific mechanisms remain elusive. Lipidomic studies have identified changes in the levels of triglycerides, phospholipids, fatty acids, and cholesterol in IPF [18,19]. For example, higher levels of lysophosphatidic acid (LPA) have been found in the blood and lung fluids of IPF patients, while other abnormalities in fatty acid metabolism have been observed [20]. Furthermore, elevated serum concentrations of small HDL particles (S-HDLPNMR) have been found to be inversely correlated with IPF risk, while lower levels of low-density lipoprotein (LDL) and cholesterol are associated with acute exacerbation IPF (AE-IPF) [21–23].

Despite these findings, the regulation of lipid metabolism in IPF at both molecular and cellular levels remains poorly understood. Signaling pathways, including HDAC8/TGFβ1/PPARG and PPARG/HMGB1/NLRP3, have been implicated in driving inflammation and fibrosis [24,25]. In addition, lipid metabolites generated following epithelial injury are taken up by macrophages, forming foam cells that further contribute to fibrotic progression [26].

Although lipid alterations and their metabolites have been linked to IPF, the precise changes in lipid-related genes and the regulatory mechanisms of lipid metabolism remain unclear. Since lipids are essential to cell membrane structure and function, they play critical roles in intracellular and extracellular signaling. However, how lipid expression varies across different cell populations in IPF and the specific pathways involved are not well understood.

To address these gaps, we conducted bioinformatics analyses of bulk and single-cell RNA-seq data from the GEO database. Our study aimed to delineate the expression profiles of lipid-related genes across different cell types involved in IPF. Furthermore, network pharmacology analysis identified potential herbal compounds capable of modulating lipid metabolism pathways as novel therapeutic avenues for IPF treatment. By elucidating lipid regulation and exploring herbal interventions, our findings contribute to a deeper understanding of IPF pathophysiology and offer new strategies for therapeutic development.

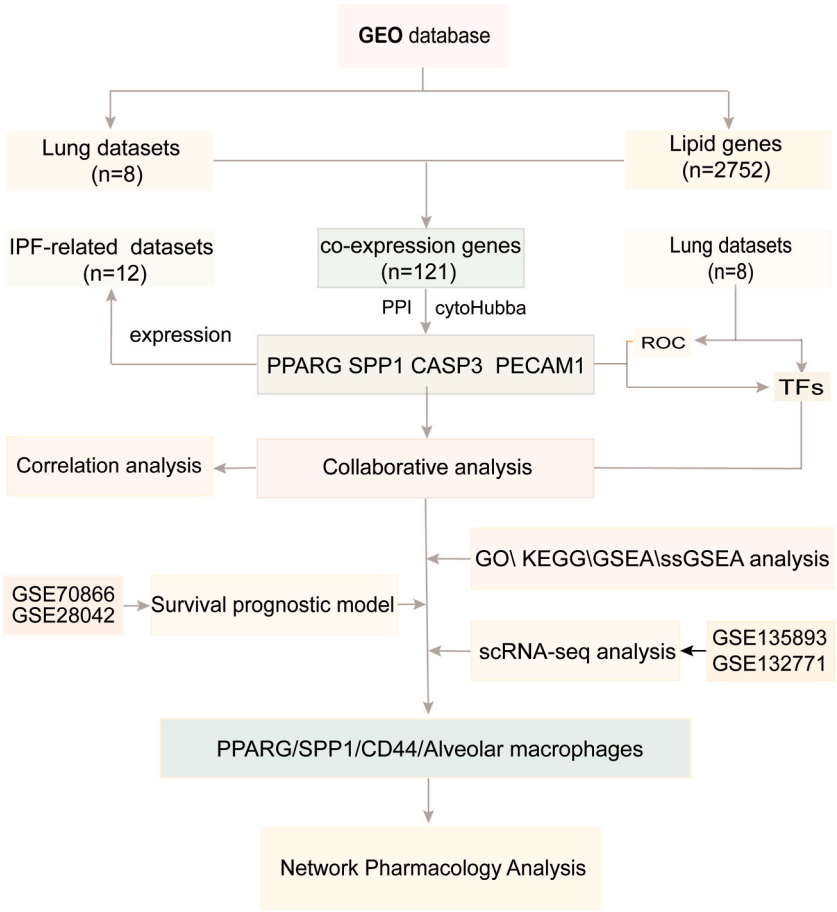

Fig. 1. Schematic of our workflow.

2. Materials and methods

2.1. Data Sources and preprocessing

Our study procedures are illustrated in Fig. 1. We accessed 12 transcriptome datasets from the GEO database, encompassing diverse sequencing platforms including Affymetrix, Agilent, and Illumina. These datasets comprised eight samples from lung tissue [(GSE175457 (GPL24676) [27], GSE150910(GPL24676) [28], GSE92592(GPL11154) [29], GSE213001(GPL21290) [30], GSE231693 (GPL20301) [31], GSE32537(GPL6244) [32], GSE110147(GPL6244) [33], GSE53845(GPL6480) [34]); three from blood samples (GSE93606(GPL11532) [35], GSE28042(GPL6480) [36], GSE38958(GPL5175) [37]); and one from bronchoalveolar lavage fluid samples (GSE70866(GPL14550-GPL17077) [38]) (Table 1). We first screened out 2754 genes associated with lipids using the keyword "lipid". Subsequently, we normalized all datasets using the R package "limma (V.3.18)" and integrated data from the same tissue and flow cell using "sva (V.3.18)" to eliminate batch effects. At significance level $P < 0.05$, significant lipid genes were identified for each lung tissue dataset. Next, we used protein-protein interaction (PPI) analysis to construct a gene interaction network, and cytoHubba (MCC, MNC, Degree, BottleNeck, Closeness, Radiality, Betweenness, Stress, and EPC) to identify the top 10 genes and take their intersection. We further assessed the expression levels of these genes across all 12 datasets. In addition, we have included single-cell RNA-seq datasets from GSE135893 [39] and GSE132771 datasets [40]. All datasets were derived from the GEO database (http://www.ncbi.nlm.nih.gov/geo/) and included IPF patient and control samples. Clinical data, such as patient survival and GAP scores, were obtained from GSE28042, GSE70866, and GSE93606.

2.2. Diagnostic models and survival prognostic analyses

Diagnostic models were developed for PPARG, SPP1, CASP3, and PECAM1 across eight lung tissue datasets using the R packages glmnet (V.4.1–8) and pROC (V.1.18.5). In the GSE70866 and GSE28042 datasets, samples were split randomly into training and test groups. To predict genes associated with survival and prognosis, we employed R packages glmnet (V.4.1–8), survival (V.3.5–7), survminer (V.0.4.9), and timeROC (V.0.4), followed by visualization analysis. All mentioned R packages can be accessed at https://cran.r-project.org/web/packages/.

2.3. Transcriptional regulation analysis

The hTFtarget database was employed to explore the transcription factors and downstream targets of PPARG, SPP1, CASP3, and PECAM1. We identified shared transcription factors for these four genes by intersecting their respective transcription factor sets. These common factors were then validated across eight lung tissue datasets to pinpoint transcription factors that were coexpressed in these samples. Spearman's correlation analysis, facilitated by Sangerbox 3.0, was subsequently used to assess the associations between these transcription factors and their target genes [41].

2.4. Enrichment analysis

Using the R package clusterProfiler (V3.18), we conducted Gene Ontology (GO) and Kyoto Encyclopedia of Genes and Genomes (KEGG) enrichment analyses, as well as gene set enrichment analysis (GSEA), and visualized the results accordingly. To assess immune infiltration, we employed single-sample gene set enrichment analysis (ssGSEA) via the R package GSVA (V.3.18). Key immune cells were identified through least absolute shrinkage and selection operator (LASSO) and support vector machines (SVM), and their correlation with the expression of the seven identified genes was examined using Spearman's correlation. For the GSE70866 and GSE93606 datasets, we utilized the R packages "survival (V.3.5.7)" and "survminer (V.0.4.9)" to analyze the association between

Table 1
Data source.

Type	Datasets	Case/N	Authors	Platform	Sequencing
Tissue	GSE175457	188/234	Borie R. et al.	GPL24676	Illumina
	GSE150910	103/103	Furusawa H. et al.	GPL24676	Illumina
	GSE213001	41/62	Jaffar J. et al.	GPL21290	Illumina
	GSE231693	20/20	Guttman A. et al.	GPL20301	Illumina
	GSE92592	19/20	LeBrasseur N. et al.	GPL11154	Illumina
	GSE32537	39/131	Yang IV. et al.	GPL6244	Affymetrix
	GSE110147	11/22	Mura M. et al.	GPL6244	Affymetrix
	GSE53845	8/40	Abbas AR. et al.	GPL6480	Agilent
Blood	GSE93606	20/154	Molyneaux PL. et al.	GPL11532	Affymetrix
	GSE28042	19/75	Herazo Maya J. et al.	GPL6480	Agilent
	GSE38958	45/70	Zhou T. et al.	GPL5175	Affymetrix
BALF	GSE70866	20/176	Prasse A. et al.	GPL14550/GPL17077	Agilent
scRNA	GSE135893	10/20	Habermann AC. et al.	GPL18573/GPL20301/GPL24676	Illumina
	GSE132771	3/3	Tsukui T. et al.	GPL21103/GPL24676	Illumina

BALF, bronchoalveolar lavage fluid; scRNA, single-cell RNA-seq.

immune cells and survival prognosis.

2.5. Analysis of single-cell datasets

We utilized the Seurat (V.5.0.1) package for data object generation and the removal of low-quality cells [42]. Standard pre-processing steps included calculating gene expression, cell counts, and mitochondrial gene percentages. Genes detected in fewer than three cells and cells expressing fewer than 500 genes or having over 20 % mitochondrial genes were excluded. The UMI counts were normalized to 10 000 to account for library size differences. Following data transformation, we applied the ScaleData function to correct for variables such as percent.mt, nCount_RNA, S.Score, G2M.Score, and nFeature_RNA through regression.

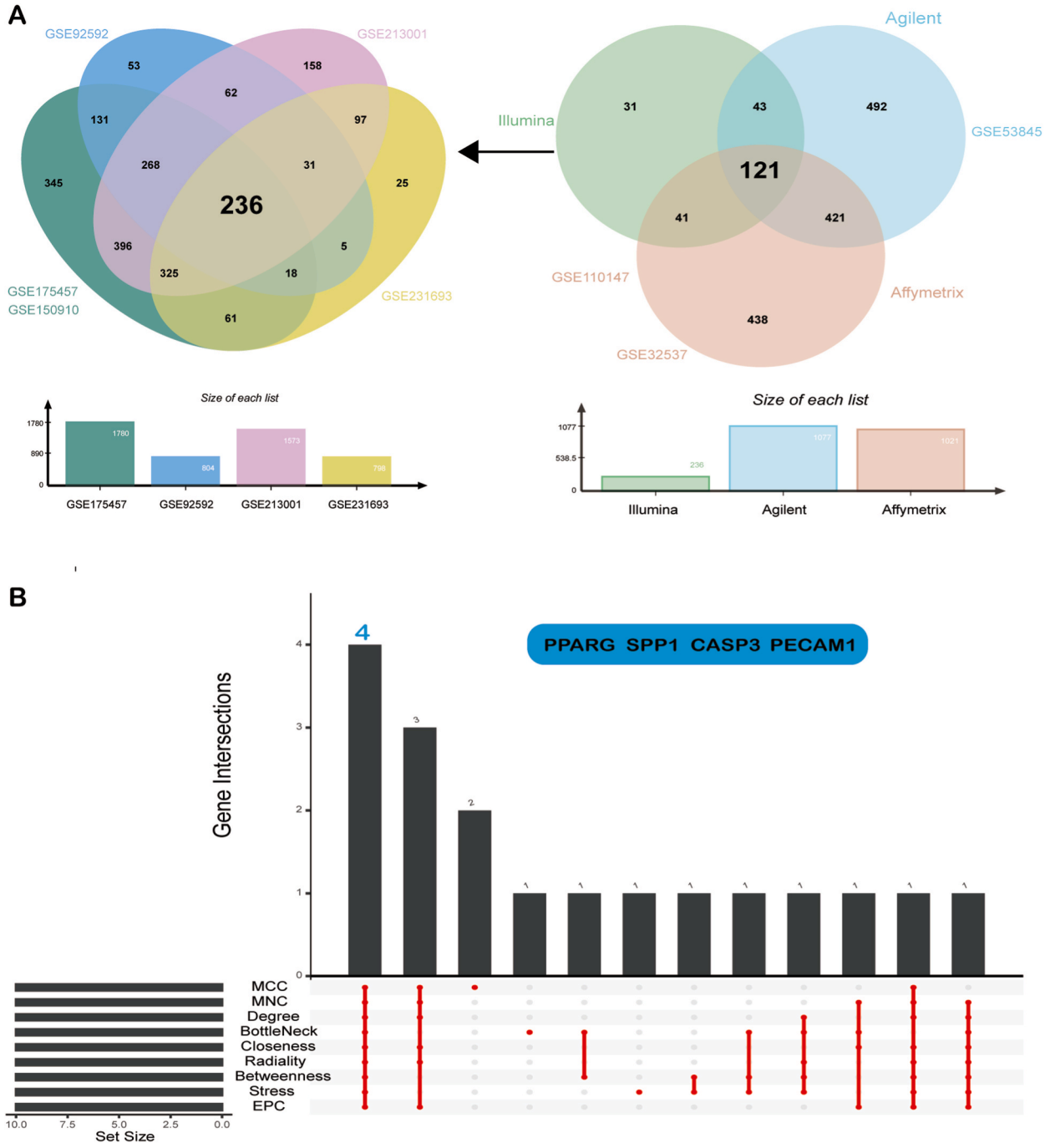

Fig. 2. 121 co-expressed lipid genes **(A)** and four core lipid genes **(B).**

For clustering and visualization, we retained the top 35 principal components and performed UMAP analysis using the RunUMAP and FindClusters functions, setting the clustering resolution at 2.5. The FindAllMarkers function was employed to identify marker genes for each cluster, and cell types were annotated using markers from the CellMarker database [43].

Differential expression analysis revealed seven genes that were significantly different between the normal and IPF groups. Additionally, CellChat (V.1.5.0) was used to analyze and visualize cell-to-cell communication, highlighting key signaling networks associated with disease progression.

2.6. Network pharmacology analysis

This study employed the Traditional Chinese Medicine Systems Pharmacology Database and Analysis Platform (TCMSP) [44] and The Encyclopedia of Traditional Chinese Medicine (ETCM) [45] databases to screen Chinese medicines and chemicals that act on PPARG. An oral bioavailability (OB) ≥20 % and a drug-like property (DL) ≥0.1 were used as screening criteria. The 3D structures of the screened compounds were subsequently then downloaded from the PubChem database, after which the ligands were removed using PyMOL software and the hydrogen atoms were added using AutoDockTools-1.5.7. Afterwards, the compounds were docked 50 times

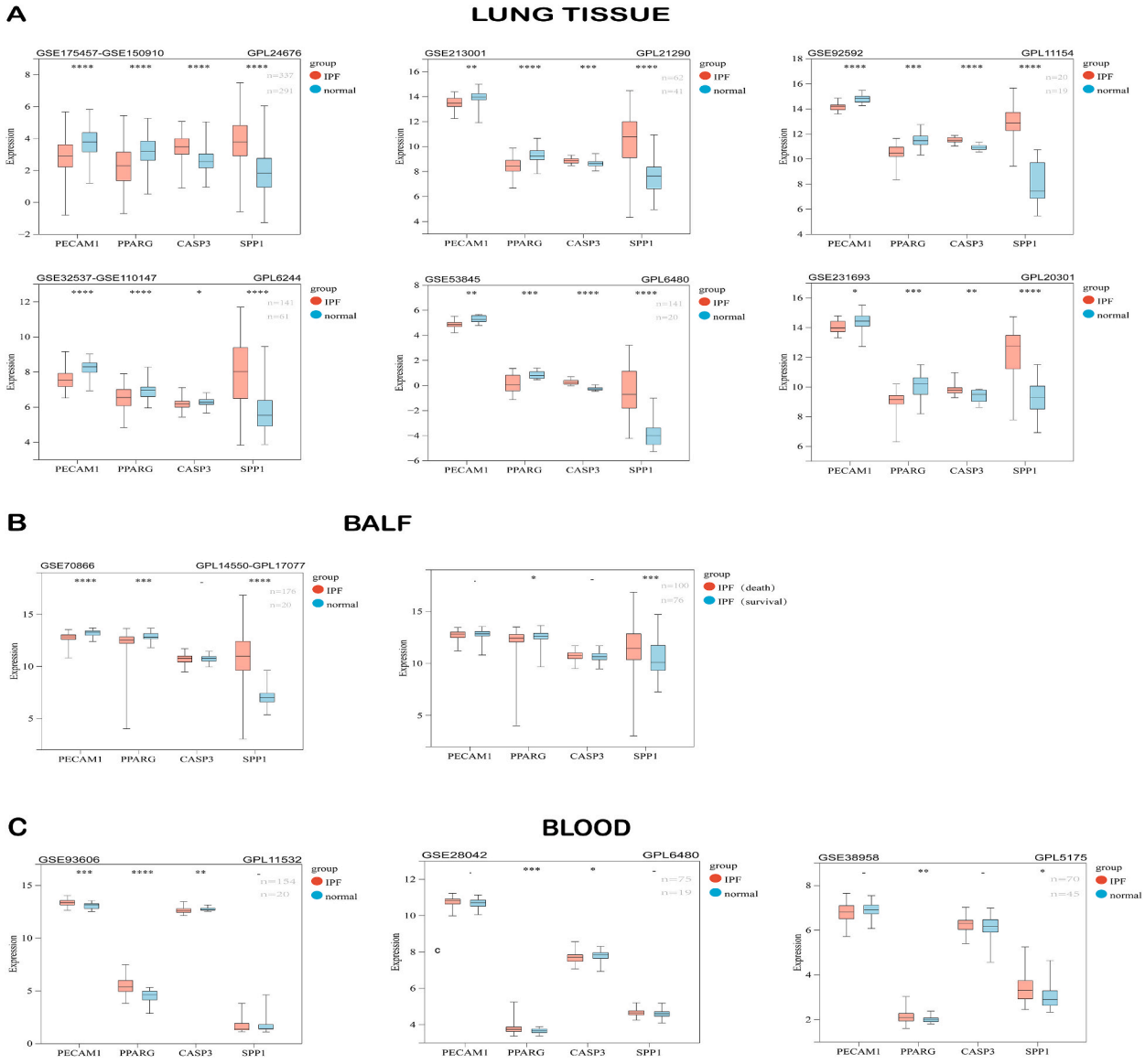

Fig. 3. Expression of PPARG, SPP1, CASP3,PECAM1 of lung tissue**(A)**, BALF**(B)** and blood**(C)** in patients with IPF. The statistical significance levels were indicated as follows: P>0.05; *P < 0.05; **P < 0.01; ***P < 0.001; ****P < 0.0001. Data sets from the same sequencing chip were merged and debatched using the SVA package, including GSE175457-GSE150910(GPL24676), GSE32537-GSE150910(GPL6244).

using AutoDock Vina, after which the minimum binding energy was used for each docking.

3. Results

3.1. Core lipid genes in IPF

By intersecting eight lung tissue datasets from Affymetrix, Agilent, and Illumina separately with the lipid genes resulted in 121 coexpressed lipid genes (Fig. 2A). After intersection analysis via protein–protein interaction (PPI) and cytoHubba analyses, four core lipid genes (PPARG, SPP1, CASP3 and PECAM1) associated with IPF were identified (Fig. 2B).

PPARG (Peroxisome Proliferator-Activated Receptor Gamma) is known to regulate lipid metabolism and has been implicated in macrophage function, which plays a key role in IPF. SPP1 (Secreted Phosphoprotein 1), a marker of macrophage activation, is crucial for cell signaling and tissue remodeling in fibrotic diseases. CASP3 (Caspase 3), an executioner of apoptosis, is involved in cell death pathways, which are often dysregulated in IPF. PECAM1 (Platelet Endothelial Cell Adhesion Molecule 1) is a vascular marker involved in endothelial function and immune cell migration, processes relevant to the vascular remodeling observed in IPF.

3.2. Expression of PPARG, SPP1, CASP3, and PECAM1

We analyzed the expression profiles of PPARG, SPP1, CASP3, and PECAM1 in idiopathic pulmonary fibrosis (IPF) across lung tissue, bronchoalveolar lavage fluid (BALF), and blood datasets. In lung tissue, both PPARG and PECAM1 were significantly downregulated, while SPP1 and CASP3 were notably upregulated, highlighting possible disruptions in lipid metabolism and apoptosis regulation

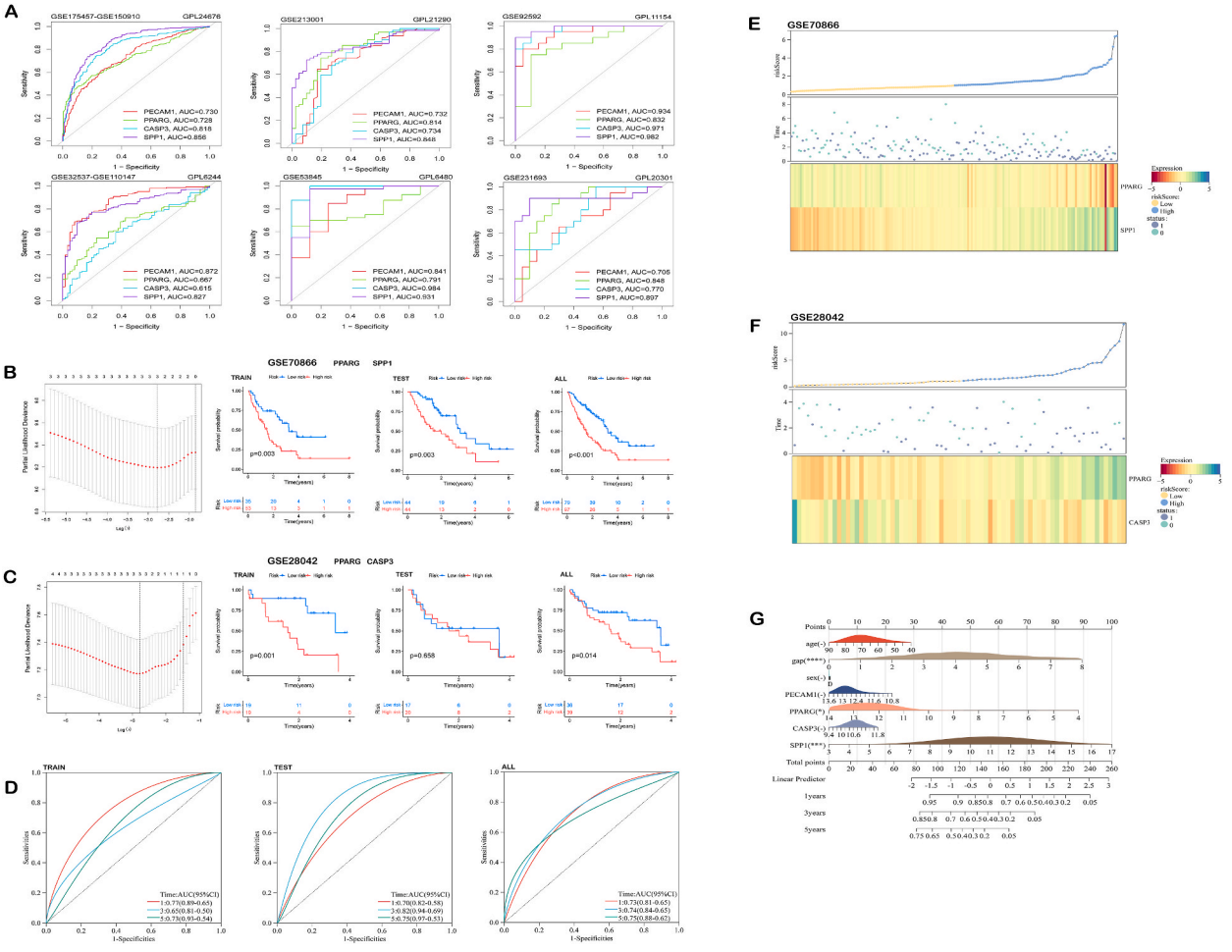

Fig. 4. ROC models were developed for PPARG, SPP1, CASP3, and PECAM1 using the lung tissue dataset**(A)**. In GSE70866, PPARG and SPP1 were identified as survival prognostic genes, predicting survival at years 1, 3 and 5**(B and D)**. In GSE70866, Correlation of PPARG and SPP1 with risk scores**(E)**. GAP is an important factor in IPF**(G)**. In GSE28042, PPARG and CASP3 were identified as survival prognostic genes**(C)**. In GSE28042, Correlation of PPARG and CASP3 with risk scores**(F)**.

(Fig. 3A). In BALF samples, the expression trends of PPARG, PECAM1, and SPP1 mirrored those observed in lung tissue, except for CASP3, where no significant difference was found (Fig. 3B). In blood samples, PPARG and PECAM1 levels were significantly elevated, suggesting a systemic response in IPF. Additionally, SPP1 was significantly upregulated in the GSE93606 dataset, whereas CASP3 exhibited no significant variation. However, in peripheral blood mononuclear cell (PBMC) datasets, CASP3 was significantly underexpressed, and no notable change was observed in SPP1 expression (Fig. 3C).

The downregulation of PPARG in lung tissue aligns with its established role in modulating lipid metabolism and anti-inflammatory processes, pointing to a potential defect in lipid regulation in IPF. Conversely, SPP1 upregulation, known for its involvement in immune responses and fibrosis, suggests an active role in fibrotic progression. The varying expression of CASP3 across tissues indicates a context-dependent role in apoptosis, while the decrease in PECAM1 expression may signal endothelial dysfunction, a key feature of IPF.

3.3. Diagnostic and survival prognostic analyses

ROC curve analysis revealed that PPARG, SPP1, CASP3, and PECAM1 have strong predictive power in diagnosing IPF, with high AUC values indicating their diagnostic efficacy (Fig. 4A). Using the LASSO algorithm on the GSE70866 and GSE2804 datasets, we identified these genes as diagnostic and survival-related markers for IPF (Fig. 4B and C).

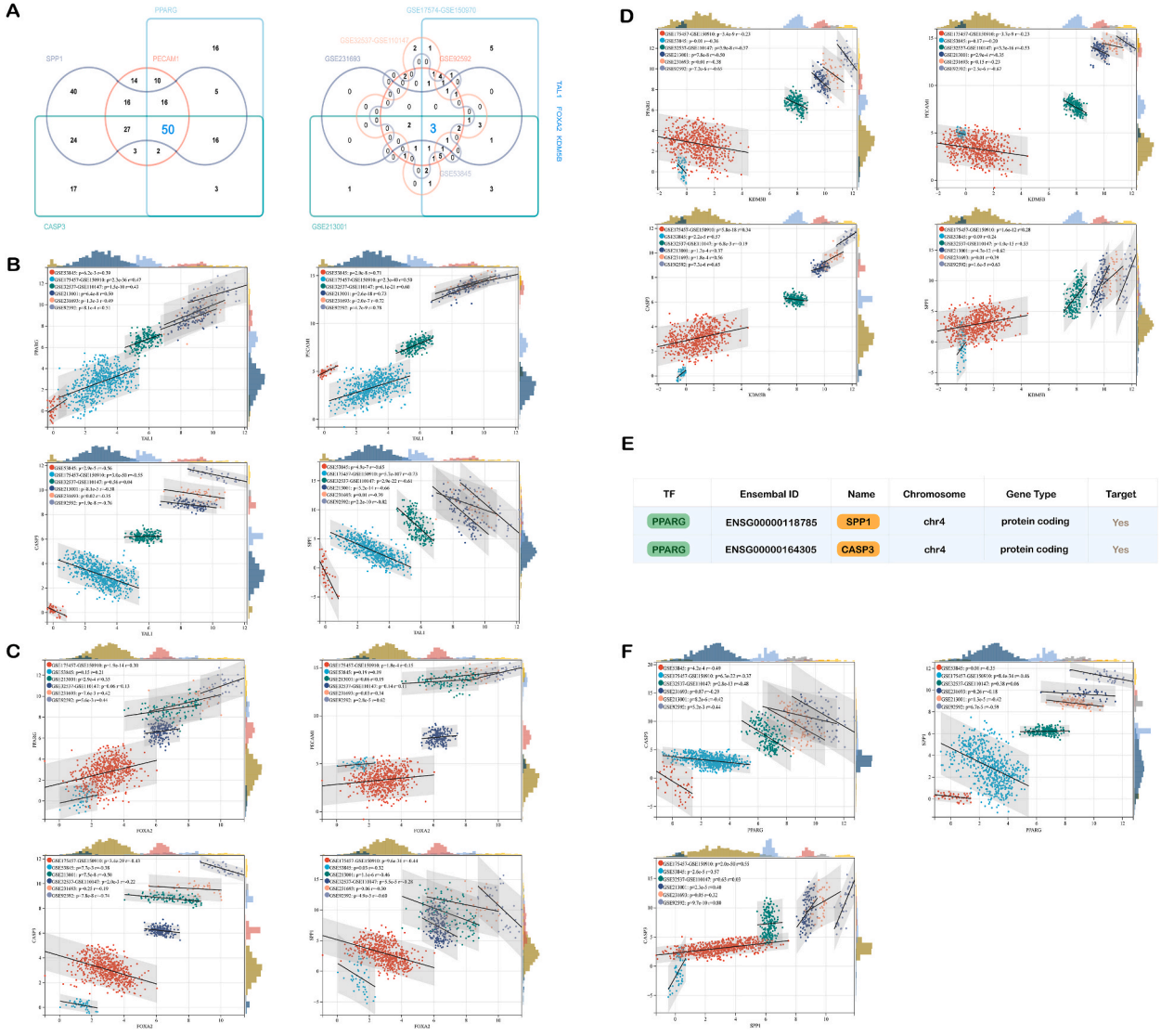

TF	Ensembal ID	Name	Chromosome	Gene Type	Target
PPARG	ENSG00000118785	SPP1	chr4	protein coding	Yes
PPARG	ENSG00000164305	CASP3	chr4	protein coding	Yes

Fig. 5. Common Transcription Factors in Lung Tissue Datasets (**A**). The correlation of TAL1 with PPARG, SPP1, CASP3, and PECAM1 (**B**). The correlation of FOXA2 with PPARG, SPP1, CASP3, and PECAM1 (**C**). The correlation of KDM5B with PPARG, SPP1, CASP3, and PECAM1 (**D**). PPARG was identified as a transcription factor for SPP1 and CASP3(**E**) The correlation of PPARG with SPP1 as well as CASP3(**F**).

PPARG, a key regulator of lipid metabolism, demonstrated protective effects in IPF, primarily through maintaining lipid homeostasis and reducing inflammation. In contrast, SPP1 and CASP3, which are involved in lipid-related signaling and apoptosis, contributed to disease progression. Survival analysis showed that low PPARG expression and high SPP1 expression were associated with poorer survival outcomes, with significant predictive power for 1-year, 3-year, and 5-year survival (Fig. 4D–. E and G).

In the GSE28042 dataset, the protective role of PPARG and the risk role of CASP3 were further validated. The risk score increased with higher PPARG expression and lower CASP3 expression. These findings, supported by existing literature, highlight PPARG's protective role through lipid metabolism regulation in lung diseases, while the dysregulation of SPP1 and CASP3 accelerates disease progression by promoting apoptosis and lipid metabolism disruption (Fig. 4F).

3.4. Analysis of the transcriptional regulation and correlation of PPARG, SPP1, CASP3, and PECAM1

We examined the transcriptional regulation of PPARG, SPP1, CASP3, and PECAM1 using hTFtarget database data. After intersecting transcription factor sequences, 50 cotranscription factors were identified, with three—KDM5B, FOXA2, and TAL1—validated in lung tissue datasets (Fig. 5A).

Correlation analysis showed that FOXA2 and TAL1 were positively associated with PPARG and PECAM1, and negatively associated with SPP1 and CASP3 (Fig. 5B and C). Conversely, KDM5B was negatively correlated with PPARG and PECAM1 and positively correlated with SPP1 and CASP3 (Fig. 5D). This suggests KDM5B may suppress lipid metabolism via PPARG while promoting apoptotic pathways through SPP1 and CASP3.

PPARG was also identified as a transcriptional regulator of SPP1 and CASP3, showing a negative correlation, indicating its potential protective role in IPF by downregulating apoptotic and inflammatory responses (Fig. 5E and F).

The discovery of KDM5B, FOXA2, and TAL1 as key regulators highlights their potential significance in IPF pathology. KDM5B, known for histone demethylation, may suppress PPARG activity, while FOXA2 and TAL1 likely support lipid homeostasis through PPARG and PECAM1 regulation.

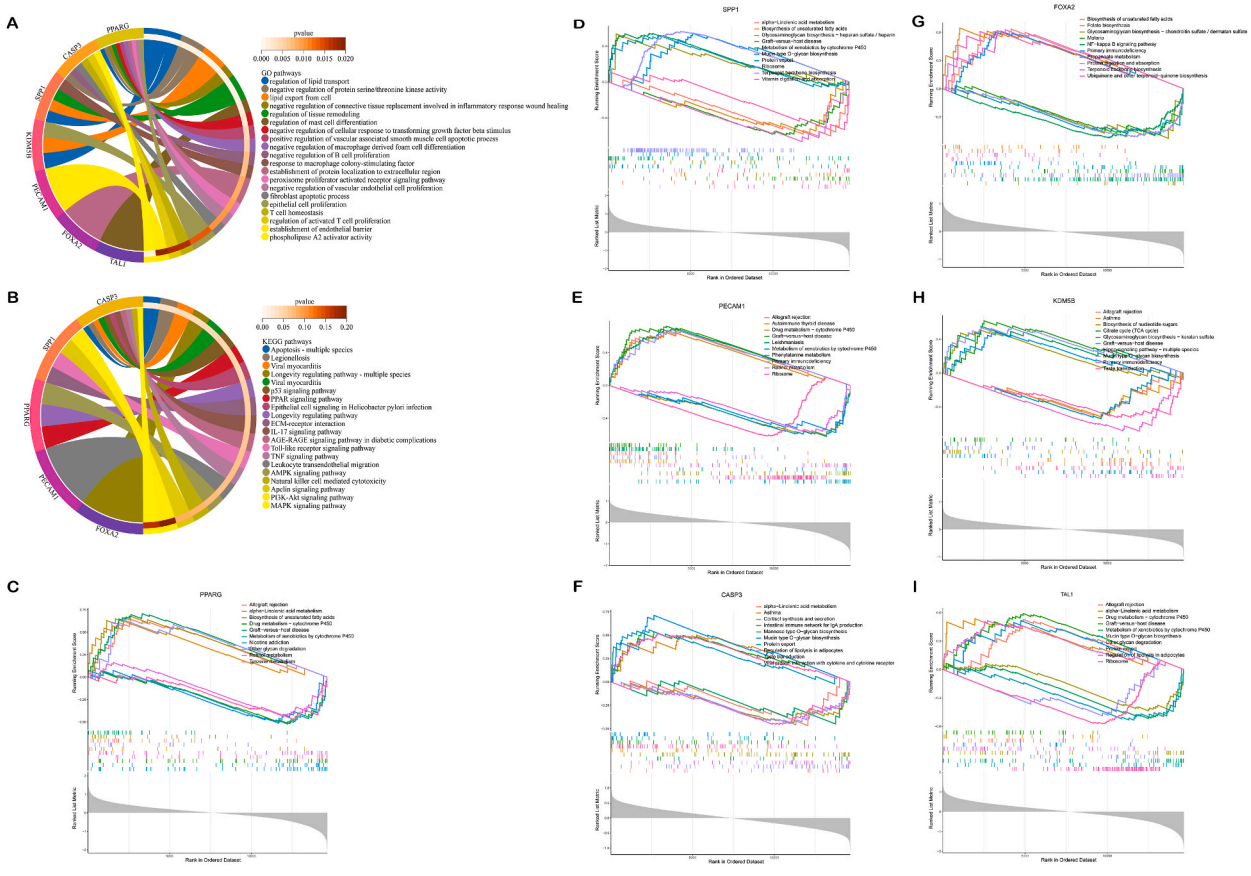

Fig. 6. Results of GO analyses**(A)**. Results of KEGG analyses**(B)**. GSEA analyses of top and bottom five signaling pathways: PPARG**(C)**; SPP1**(D)**; PECAM1 **(E)**; CASP3**(F)**; FOXA2**(G)**; KDM5B**(H)**; TAL1(**I**).

3.5. Enrichment analysis results

Enrichment analyses for PPARG, SPP1, CASP3, PECAM1, KDM5B, FOXA2, and TAL1 revealed significant biological pathways associated with lipid transport regulation, apoptosis, connective tissue repair, and inflammatory response (Fig. 6A and B). Key GO terms and KEGG pathways highlighted processes such as lipid metabolism and the regulation of apoptosis, which are critical in IPF progression. The GSEA analysis also identified relevant pathways, including alpha-linolenic acid metabolism, cytochrome P450-related drug metabolism, and biosynthesis of unsaturated fatty acids (Fig. 6C–I). These pathways provide insight into how metabolic dysfunction, immune response, and tissue repair may contribute to IPF pathology.

Using ssGSEA, Lasso, and SVM algorithms, we identified key immune cells, including macrophages, neutrophils, and T-helper cells, that showed differential expression in IPF). Correlation analysis revealed that PPARG was positively correlated with macrophages, while SPP1 showed a negative correlation. In lung tissue, activated dendritic cells and Th17 cells were downregulated (Fig. 7A–E), while in BALF and blood, macrophages, neutrophils, and mast cells were upregulated (Fig. 8A–E and Fig. 9A–E). These immune cell dynamics suggest a link between immune regulation and disease progression.

Further survival analysis showed that high levels of macrophages, neutrophils, and regulatory T cells were associated with poorer patient survival outcomes (Fig. 8F–H). Conversely, central memory CD4 T cells were correlated with better survival prospects (Fig. 9F–H). Notably, PPARG and SPP1 played opposing roles in regulating macrophages across lung tissue, BALF, and blood samples, reinforcing their distinct contributions to immune modulation and disease progression in IPF.

3.6. Single-cell sequencing analysis

After normalizing the single-cell data, cellular annotation was performed, revealing distinct gene expression patterns across cell types (Fig. 10A). PPARG and SPP1 were predominantly expressed in alveolar macrophages (AMs), with FOXA2 in AT1 cells, TAL1 in endothelial and mast cells, KDM5B in basal cells, PECAM1 in endothelial cells, and CASP3 in NK cells (Fig. 10B). Compared with normal populations, IPF patients exhibited reduced PPARG expression and elevated SPP1 expression in AMs. FOXA2 was downregulated in AT1 cells but upregulated in AT2 cells, while KDM5B showed minimal expression in basal cells. TAL1 and PECAM1 were

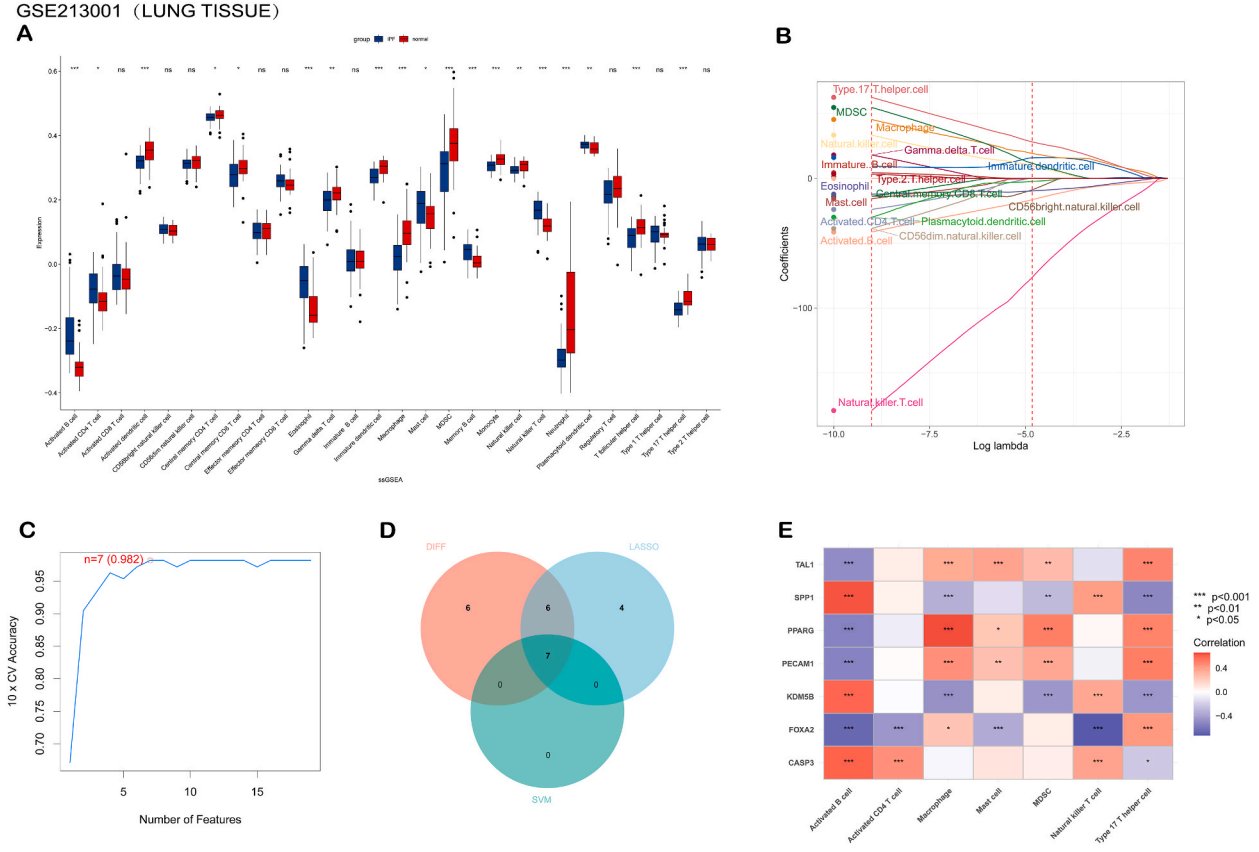

Fig. 7. Lung tissue dataset (GSE213001). Results of ssGSEA analyses**(A)**. Lasso predicts core immune cells**(B)**. Accuracy of SVM algorithms for predicting core immune cells **(C)**. Core immune cell intersections**(D).** Seven genes correlate with core immune cells**(E).** The statistical significance levels were indicated as follows: P>0.05; *P < 0.05; **P < 0.01; ***P < 0.001; ****P < 0.0001.

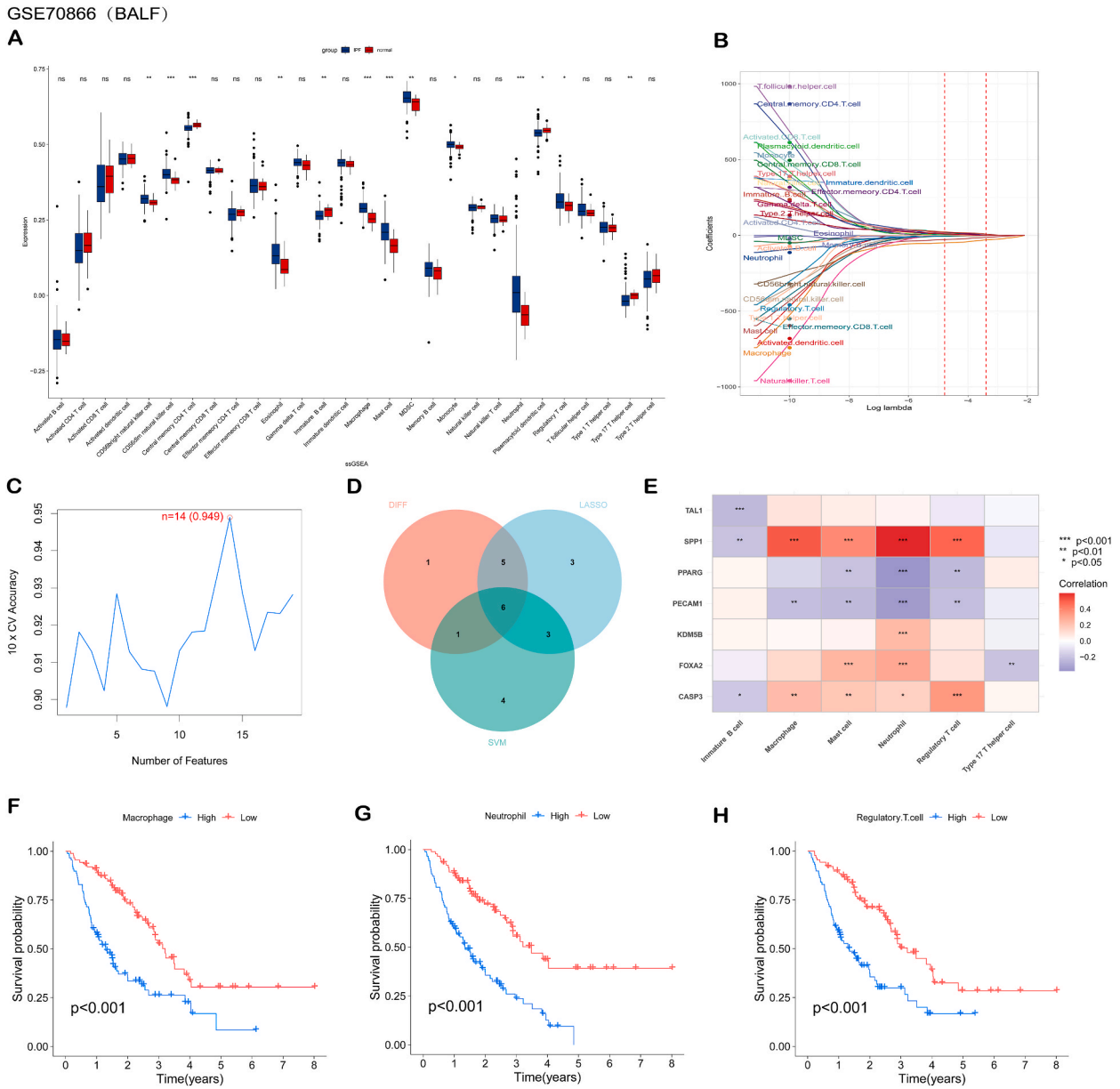

Fig. 8. BALF dataset (GSE70866). Results of ssGSEA analyses**(A).** Lasso predicts core immune cells**(B).** Accuracy of SVM algorithms for predicting core immune cells **(C).** Core immune cell intersections**(D).** Seven genes correlate with core immune cells**(E).** Immune cells associated with survival **(F-H).** The statistical significance levels were indicated as follows: P>0.05; *P < 0.05; **P < 0.01; ***P < 0.001; ****P < 0.0001.

both expressed at low levels in vascular endothelial cells, and CASP3 expression was decreased in NK cells (Fig. 10C). Significantly altered cell populations were observed in IPF, with decreased proportions of alveolar and interstitial macrophages, monocytes, T cells, vascular endothelial cells, and AT2 cells. Conversely, plasma cells, B cells, dendritic cells, fibroblasts, club cells, and ciliated cells were increased (Fig. 10D).

Intercellular signaling analysis revealed that specific pathways were activated in IPF, including HGF, CD34, EDN, CD40, CD6, ALCAM, THY1, SPP1, and CXCL signaling pathways, whereas ANXA1, CD22, ANGPT, and others were more active in the normal group (Fig. 10E). Both IPF and normal groups shared activation of the PECAM1 signaling pathway. In the SPP1 pathway, alveolar macrophages, pulmonary intravascular macrophages, and B cells acted as key signal transmitters, receivers, and mediators (Fig. 10F–. H, Fig. 10J and K). For the PECAM1 pathway, lymphatic and vascular endothelial cells, along with pulmonary macrophages, played central roles (Fig. 10G and I).

The altered expression of PPARG and SPP1 in AMs underscores their involvement in lipid metabolism and immune regulation, particularly in the inflammatory and fibrotic environment of IPF. SPP1, acting through CD44, likely contributes to the pro-fibrotic

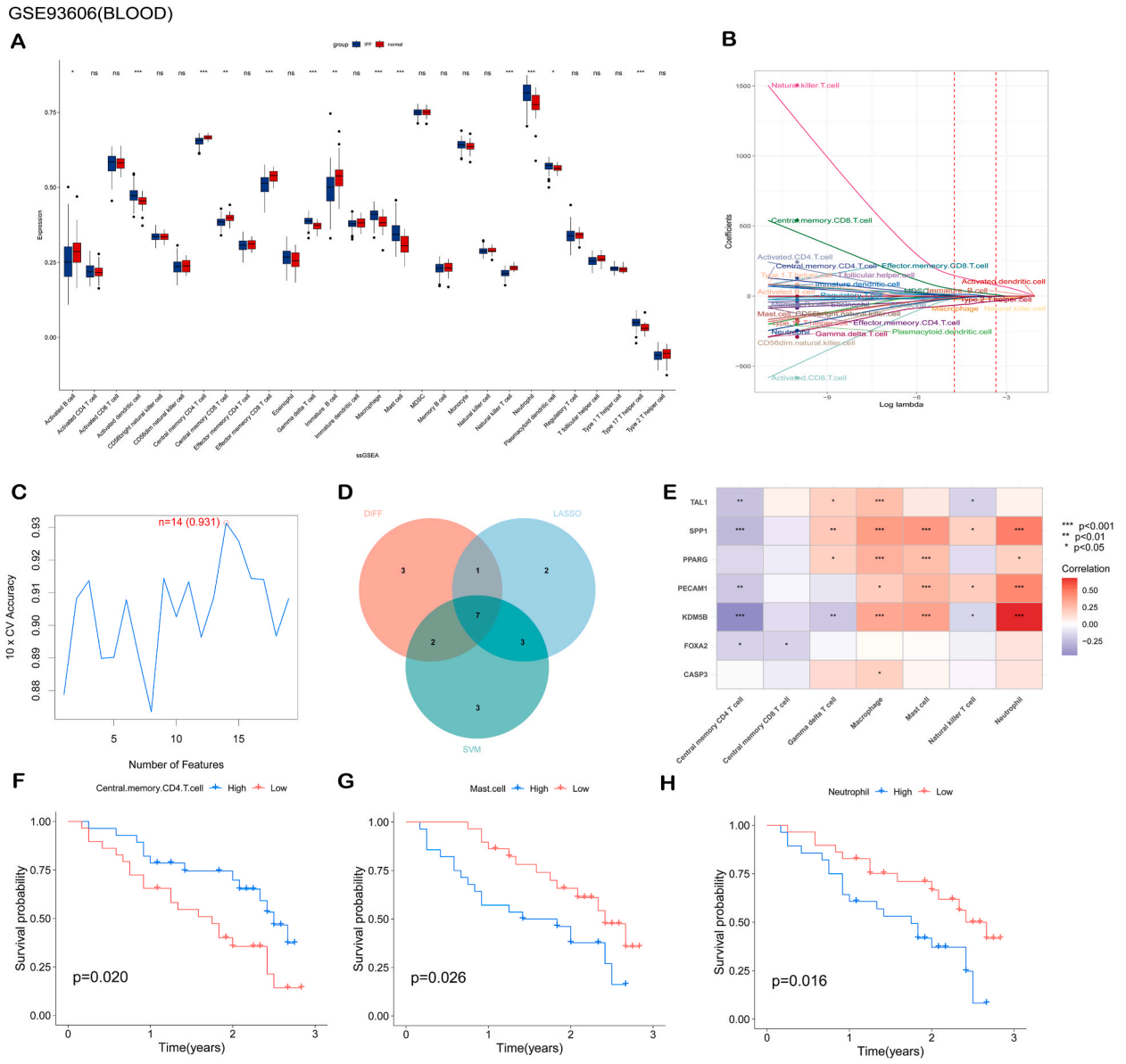

Fig. 9. BLOOD dataset (GSE93606). Results of ssGSEA analyses**(A)**. Lasso predicts core immune cells**(B)**. Accuracy of SVM algorithms for predicting core immune cells **(C)**. Core immune cell intersections**(D).** Seven genes correlate with core immune cells**(E).** Immune cells associated with survival **(F-H).** The statistical significance levels were indicated as follows: P>0.05; *P < 0.05; **P < 0.01; ***P < 0.001; ****P < 0.0001.

signaling observed in the disease, while the downregulation of PPARG may reflect disrupted lipid metabolism, a key feature of IPF pathology.

3.7. *Network pharmacology analysis*

Using the TCMSP and ETCM databases, we screened 346 herbs and 17 classes of compounds with potential effects on PPARG (Fig. 11A). Among them, five herbs—*Carthami Flos*, *Ginkgo Folium*, *Portulacae Herba*, *Phyllanthi Fructus*, and *Ephedra Herba*—were identified as containing the most bioactive compounds (Fig. 11B). Molecular docking analyses further confirmed the strong binding affinity of these compounds with PPARG (Fig. 11C–S).

Recent studies suggest that herbs play a critical role in combatting organ fibrosis. For example, *Carthami Flos* has been shown to inhibit angiogenesis and alleviate hepatic fibrosis [46], myocardial fibrosis [47], and renal fibrosis [48]. Similarly, *Ginkgo Folium* demonstrates protective effects against pulmonary and hepatic fibrosis via the Akt/mTOR signaling pathway [49–51]. Additionally, *Portulacae Herba* inhibits the TLR-4/NF-κB, Bcl-2/Bax, and TGF-β1/Smad2 pathways to combat liver fibrosis [52], while *Ephedra Herba*

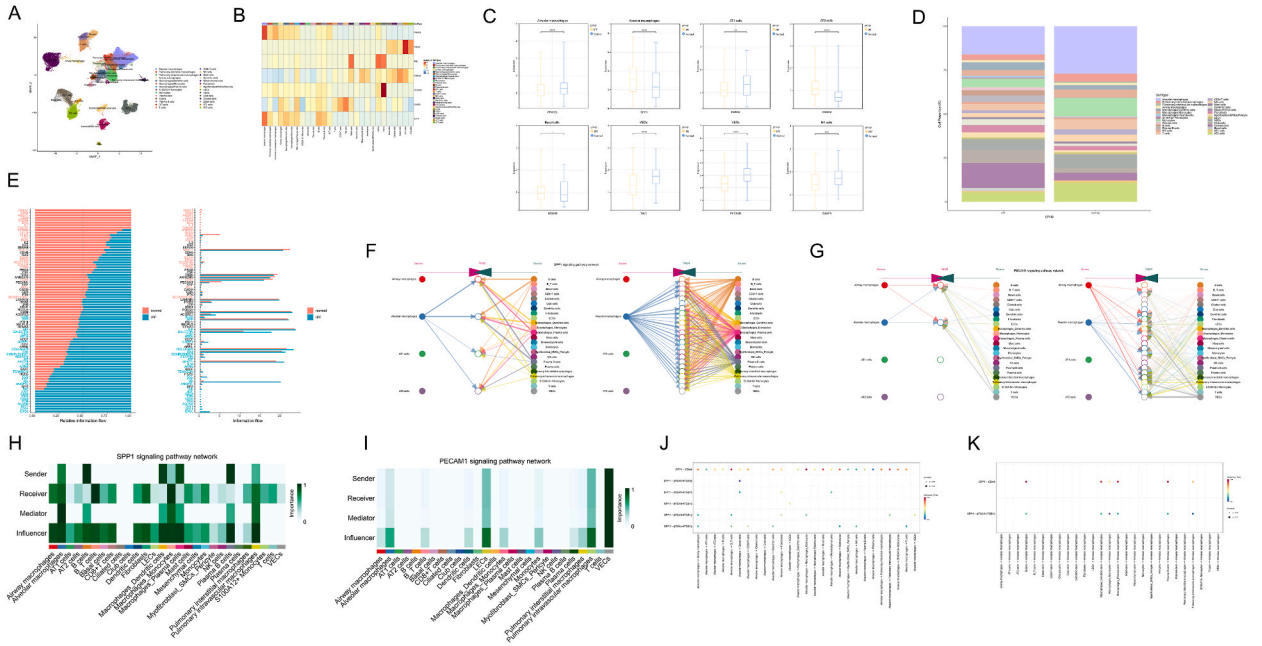

Fig. 10. Cellular swarming**(A).** Heat map of the seven genes**(B).** Differences in expression of seven genes between normal and IPF groups of highly expressed cells**(C).** Relative proportion of different cells between normal and IPF groups**(D).** Signaling pathways between normal and IPF groups**(E).** SPP1 signaling pathway network **(F and H)**. PECAM1 signaling pathway network **(G and I)**. Targets of interaction between alveolar macrophages and other cells**(J).** Targets of interaction between other cells and alveolar macrophages**(K).**

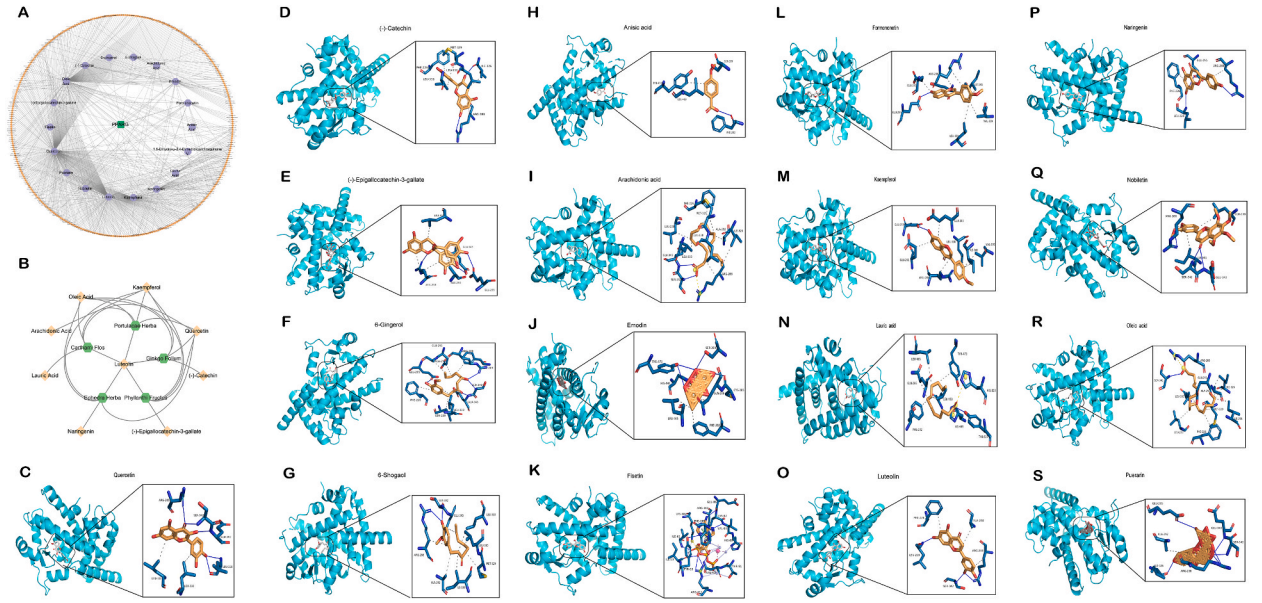

Fig. 11. 346 herbs and 17 botanicals**(A).** 5 Herbs with the Most Active Ingredients**(B).** Molecular docking results: Quercetin**(C)**; (−)-Catechin**(D)**; (−)-Epigallocatechin-3-gallate**(E)**; 6-Gingerol**(F)**; 6-Shogaol**(G)**; Anisic acid**(H)**; Arachidonic acid**(I)**; Emodin**(J)**; Fisetin**(K)**; Formononetin**(L)**; Kaempferol**(M)**; Lauric acid**(N)**; Luteolin**(O)**; Naringenin**(P)**; Nobiletin**(Q)**; Oleic acid**(R)**; Puerarin**(S)**.

mitigates fibrosis by inhibiting alveolar epithelial-mesenchymal transition and promoting autophagy [53]. *Ephedra* combined with *Schisandrae Chinensis Fructus* has been shown to reduce alveolar inflammation and pulmonary fibrosis [54].

In the context of IPF, the molecular docking results suggest that these herbs, through their bioactive compounds, may modulate PPARG activity to reduce fibrosis. This highlights their potential as alternative or adjunct therapies for pulmonary fibrosis.

4. Discussion

Lipid metabolism plays a pivotal role in the pathogenesis of IPF, particularly in alveolar macrophages (AMs), which are critical for lung homeostasis. In this study, we identified four key genes—PPARG, SPP1, CASP3, and PECAM1—that are significantly dysregulated in IPF lung tissue. Notably, our analysis highlighted the PPARG/SPP1/CD44 signaling pathway as a novel and central signaling pathway in regulating lipid metabolism within AMs. This study provides new insights into the molecular mechanisms underlying IPF and opens potential avenues for targeted therapies.

Our findings indicate that PPARG, a transcription factor vital for lipid metabolism and energy homeostasis, is significantly downregulated in IPF lung tissue and AMs, while SPP1 is highly expressed. PPARG, known for its anti-fibrotic properties [55–58]. positively regulates SPP1 and CASP3, suggesting a complex regulatory network that impacts lipid accumulation and fibrosis in the lung. In AMs, PPARG mediates the uptake and metabolism of lipids, and its downregulation may contribute to the formation of "foamy" AMs, which are linked to fibrosis progression [59–61]. SPP1, on the other hand, interacts with CD44, facilitating intercellular signaling that promotes fibrosis via EMT pathway [62]. This PPARG/SPP1/CD44 signaling pathway is thus crucial for understanding lipid dysregulation in IPF and its role in driving disease progression.

One key observation from our study is the differential expression of PPARG in lung tissue versus blood. While low in lung tissue, PPARG expression was elevated in the blood of IPF patients, suggesting a compensatory mechanism where monocytes differentiate into AMs to replenish those lost through apoptosis [61]. This dynamic between lung and blood PPARG levels underscores its central role in AM survival and lipid homeostasis [55].

SPP1 was also found to be highly expressed in both lung tissue and bronchoalveolar lavage fluid (BALF) in IPF patients, as well as in the BLM-induced mouse model of fibrosis [63,64]. SPP1 has been established as a marker of fibroblast activation, and high expression of SPP1 in macrophages and fibroblasts further drives fibrotic processes in IPF [65,66]. The interaction of SPP1 with CD44 has been shown to activate signaling cascades that promote epithelial-mesenchymal transition (EMT), a key event in fibrosis development [67]. Importantly, our transcriptional regulation analysis revealed that PPARG is an upstream negative regulator of SPP1, adding a new layer of understanding to the pathophysiology of IPF. The PPARG/SPP1/CD44 signaling pathway, therefore, emerges as a core pathway in the regulation of lipid metabolism in AMs during IPF progression. The low expression of PPARG and high expression of SPP1 drive a feedback loop that fuels fibrosis, with CD44 acting as a critical mediator of cell-cell communication [68]. Given these findings, targeting the PPARG/SPP1/CD44 signaling pathway presents a promising therapeutic strategy for modulating lipid metabolism and potentially alleviating IPF symptoms.

CASP3, typically associated with apoptosis [69,70], was also highly expressed in our IPF samples. Its activation in AMs may be linked to autophagy defects and cell death, further disrupting lipid metabolism and limiting the ability of AMs to clear deposited lipids. This imbalance in lipid metabolism is likely a contributing factor to the pathology of IPF, as AMs fail to effectively remove excess lipids, exacerbating inflammation and fibrosis.

In exploring therapeutic approaches, our study identified several herbal compounds, including Carthami Flos, Ginkgo Folium, and Ephedra Herba, which may exert anti-fibrotic effects through modulation of PPARG. These compounds have shown potential in other models of fibrosis, suggesting their utility as complementary treatments for IPF. However, further preclinical and clinical studies are required to confirm their efficacy in IPF patients.

Limitations of this study include the small sample size of publicly available datasets, which may limit the generalizability of our findings. Additionally, the lack of detailed patient survival data in these datasets constrains our ability to correlate molecular signatures with clinical outcomes. Moreover, while our network pharmacology analysis suggests potential therapeutic compounds, their clinical relevance remains uncertain until validated through rigorous preclinical and clinical studies.

In conclusion, although we propose that the PPARG/SPP1/CD44 signaling pathway plays a critical role in lipid metabolism dysregulation in AMs, contributing to IPF progression, translating these findings into clinical applications will require further experimental validation and clinical trials. Future research should focus on testing the therapeutic potential of targeting this axis, particularly with herbal compounds that modulate PPARG activity in IPF.

CRediT authorship contribution statement

Ganggang Li: Writing – original draft, Resources, Project administration, Methodology, Investigation, Funding acquisition, Data curation. **Yuwei Zhang:** Writing – original draft, Software, Formal analysis, Data curation, Conceptualization. **Huanyu Jiang:** Writing – review & editing, Visualization, Methodology, Data curation. **Xuanyu Wu:** Visualization, Data curation. **Yanwei Hao:** Validation, Software. **Yuchen Su:** Validation, Data curation. **Yutong Zou:** Software. **Wenjia Xian:** Investigation, Data curation. **Fei Wang:** Writing – original draft, Supervision. **Quanyu Du:** Writing – review & editing, Supervision, Funding acquisition.

Institutional review board statement

“Not applicable” for studies not involving humans or animals.

Data availability

The datasets used in the manuscript are publicly available.

Funding sources

This work was supported by the National Natural Science Foundation of China (grant no. 82104829; 82174347) and Science and Technology Plan Project of Sichuan Province (grant no. 2023JDRC0092).

Declaration of competing interest

The authors declare that they have no known competing financial interests or personal relationships that could have appeared to influence the work reported in this paper.

Acknowledgments

We would like to thank Nan Jia and Xueqing Duan for helping us with this work.

Appendix A. Supplementary data

Supplementary data to this article can be found online at https://doi.org/10.1016/j.heliyon.2025.e41628.

References

[1] D.J. Lederer, F.J. Martinez, Idiopathic pulmonary fibrosis, N. Engl. J. Med. 378 (19) (2018) 1811–1823.
[2] F.J. Martinez, H.R. Collard, A. Pardo, et al., Idiopathic pulmonary fibrosis, Nat. Rev. Dis. Prim. 3 (2017) 17074.
[3] D. Okuno, N. Sakamoto, Y. Akiyama, et al., Two distinct mechanisms underlying γδ T cell-mediated regulation of collagen type I in lung fibroblasts, Cells 11 (18) (2022).
[4] V.J. Thannickal, Y. Zhou, A. Gaggar, et al., Fibrosis: ultimate and proximate causes, J. Clin. Invest. 124 (11) (2014) 4673–4677.
[5] J. Behr, A. Prasse, H. Wirtz, et al., Survival and course of lung function in the presence or absence of antifibrotic treatment in patients with idiopathic pulmonary fibrosis: long-term results of the INSIGHTS-IPF registry, Eur. Respir. J. 56 (2) (2020).
[6] L. Richeldi, R.M. Du Bois, G. Raghu, et al., Efficacy and safety of nintedanib in idiopathic pulmonary fibrosis, N. Engl. J. Med. 370 (22) (2014) 2071–2082.
[7] T.E. King Jr., W.Z. Bradford, S. Castro-Bernardini, et al., A phase 3 trial of pirfenidone in patients with idiopathic pulmonary fibrosis, N. Engl. J. Med. 370 (22) (2014) 2083–2092.
[8] Y. Dotan, A. Vaidy, W.B. Shapiro, et al., Effect of acute exacerbation of idiopathic pulmonary fibrosis on lung transplantation outcome, Chest 154 (4) (2018) 818–826.
[9] Z. Wu, R. Shi, S. Yan, et al., Integrating network pharmacology, experimental validation and molecular docking to reveal the alleviation of Yinhuang granule on idiopathic pulmonary fibrosis, Phytomedicine 128 (2024) 155368.
[10] H. Li, C. Zhao, G. Muhetaer, et al., Integrated RNA-sequencing and network pharmacology approach reveals the protection of Yiqi Huoxue formula against idiopathic pulmonary fibrosis by interfering with core transcription factors, Phytomedicine 104 (2022) 154301.
[11] J. Schipke, D. Jütte, C. Brandenberger, et al., Dietary carbohydrates and fat induce distinct surfactant alterations in mice, Am. J. Respir. Cell Mol. Biol. 64 (3) (2021) 379–390.
[12] V. Suryadevara, R. Ramchandran, D.W. Kamp, et al., Lipid mediators regulate pulmonary fibrosis: potential mechanisms and signaling pathways, Int. J. Mol. Sci. 21 (12) (2020).
[13] W. Roque, F. Romero, Cellular metabolomics of pulmonary fibrosis, from amino acids to lipids, Am. J. Physiol. Cell Physiol. 320 (5) (2021) C689–c695.
[14] G. Wang, M. Qiu, X. Xing, et al., Lung cancer scRNA-seq and lipidomics reveal aberrant lipid metabolism for early-stage diagnosis, Sci. Transl. Med. 14 (630) (2022) eabk2756.
[15] E.D. Telenga, R.F. Hoffmann, T.K. Ruben, et al., Untargeted lipidomic analysis in chronic obstructive pulmonary disease. Uncovering sphingolipids, Am. J. Respir. Crit. Care Med. 190 (2) (2014) 155–164.
[16] Q. Ye, N. Barrett, B. Balestrieri, Bioactive lipids: accessible indicators toward improved diagnosis and treatment of asthma, J. Allergy Clin. Immunol. 150 (4) (2022) 790–792.
[17] C.C. Silliman, N.F. Voelkel, J.D. Allard, et al., Plasma and lipids from stored packed red blood cells cause acute lung injury in an animal model, J. Clin. Invest. 101 (7) (1998) 1458–1467.
[18] S. Nambiar, B. Clynick, B.S. How, et al., There is detectable variation in the lipidomic profile between stable and progressive patients with idiopathic pulmonary fibrosis (IPF), Respir. Res. 22 (1) (2021) 105.
[19] J. Weckerle, S. Picart-Armada, S. Klee, et al., Mapping the metabolomic and lipidomic changes in the bleomycin model of pulmonary fibrosis in young and aged mice, Dis Model Mech 15 (1) (2022).
[20] S.B. Montesi, S.K. Mathai, L.N. Brenner, et al., Docosatetraenoyl LPA is elevated in exhaled breath condensate in idiopathic pulmonary fibrosis, BMC Pulm. Med. 14 (2014) 5.
[21] A.V. Barochia, M. Kaler, N. Weir, et al., Serum levels of small HDL particles are negatively correlated with death or lung transplantation in an observational study of idiopathic pulmonary fibrosis, Eur. Respir. J. 58 (6) (2021).
[22] R. Chen, J. Dai, Lipid metabolism in idiopathic pulmonary fibrosis: from pathogenesis to therapy, J. Mol. Med. (Berl.) 101 (8) (2023) 905–915.
[23] Y. Hachisu, K. Murata, K. Takei, et al., Possible serological markers to predict mortality in acute exacerbation of idiopathic pulmonary fibrosis, Medicina 55 (5) (2019).
[24] S. Yang, Y. Sun, Y. Luo, et al., Hypermethylation of PPARG-encoding gene promoter mediates fine particulate matter-induced pulmonary fibrosis by regulating the HMGB1/NLRP3 axis, Ecotoxicol. Environ. Saf. 272 (2024) 116068.
[25] S. Saito, Y. Zhuang, T. Suzuki, et al., HDAC8 inhibition ameliorates pulmonary fibrosis, Am. J. Physiol. Lung Cell Mol. Physiol. 316 (1) (2019) L175–l186.
[26] F. Romero, D. Shah, M. Duong, et al., A pneumocyte-macrophage paracrine lipid axis drives the lung toward fibrosis, Am. J. Respir. Cell Mol. Biol. 53 (1) (2015) 74–86.
[27] R. Borie, J. Cardwell, I.R. Konigsberg, et al., Colocalization of gene expression and DNA methylation with genetic risk variants supports functional roles of MUC5B and DSP in idiopathic pulmonary fibrosis, Am. J. Respir. Crit. Care Med. 206 (10) (2022) 1259–1270.
[28] H. Furusawa, J.H. Cardwell, T. Okamoto, et al., Chronic hypersensitivity pneumonitis, an interstitial lung disease with distinct molecular signatures, Am. J. Respir. Crit. Care Med. 202 (10) (2020) 1430–1444.
[29] M.J. Schafer, T.A. White, K. Iijima, et al., Cellular senescence mediates fibrotic pulmonary disease, Nat. Commun. 8 (2017) 14532.

[30] J. Jaffar, M. Wong, G.A. Fishbein, et al., Matrix metalloproteinase-7 is increased in lung bases but not apices in idiopathic pulmonary fibrosis, ERJ Open Res 8 (4) (2022).
[31] G. Jia, T.R. Ramalingam, J.V. Heiden, et al., An interleukin 6 responsive plasma cell signature is associated with disease progression in systemic sclerosis interstitial lung disease, iScience 26 (11) (2023) 108133.
[32] I.V. Yang, C.D. Coldren, S.M. Leach, et al., Expression of cilium-associated genes defines novel molecular subtypes of idiopathic pulmonary fibrosis, Thorax 68 (12) (2013) 1114–1121.
[33] M.J. Cecchini, K. Hosein, C.J. Howlett, et al., Comprehensive gene expression profiling identifies distinct and overlapping transcriptional profiles in non-specific interstitial pneumonia and idiopathic pulmonary fibrosis, Respir. Res. 19 (1) (2018) 153.
[34] D.J. Depianto, S. Chandriani, A.R. Abbas, et al., Heterogeneous gene expression signatures correspond to distinct lung pathologies and biomarkers of disease severity in idiopathic pulmonary fibrosis, Thorax 70 (1) (2015) 48–56.
[35] P.L. Molyneaux, S. a G. Willis-Owen, M.J. Cox, et al., Host-microbial interactions in idiopathic pulmonary fibrosis, Am. J. Respir. Crit. Care Med. 195 (12) (2017) 1640–1650.
[36] Y. Huang, S.F. Ma, R. Vij, et al., A functional genomic model for predicting prognosis in idiopathic pulmonary fibrosis, BMC Pulm. Med. 15 (2015) 147.
[37] L.S. Huang, B. Mathew, H. Li, et al., The mitochondrial cardiolipin remodeling enzyme lysocardiolipin acyltransferase is a novel target in pulmonary fibrosis, Am. J. Respir. Crit. Care Med. 189 (11) (2014) 1402–1415.
[38] A. Prasse, H. Binder, J.C. Schupp, et al., BAL cell gene expression is indicative of outcome and airway basal cell involvement in idiopathic pulmonary fibrosis, Am. J. Respir. Crit. Care Med. 199 (5) (2019) 622–630.
[39] A.C. Habermann, A.J. Gutierrez, L.T. Bui, et al., Single-cell RNA sequencing reveals profibrotic roles of distinct epithelial and mesenchymal lineages in pulmonary fibrosis, Sci. Adv. 6 (28) (2020) eaba1972.
[40] T. Tsukui, K.H. Sun, J.B. Wetter, et al., Collagen-producing lung cell atlas identifies multiple subsets with distinct localization and relevance to fibrosis, Nat. Commun. 11 (1) (2020) 1920.
[41] W. Shen, Z. Song, X. Zhong, et al., Sangerbox: a comprehensive, interaction-friendly clinical bioinformatics analysis platform, iMeta 1 (3) (2022) e36.
[42] T. Stuart, A. Butler, P. Hoffman, et al., Comprehensive integration of single-cell data, Cell 177 (7) (2019) 1888–1902.e21.
[43] X. Zhang, Y. Lan, J. Xu, et al., CellMarker: a manually curated resource of cell markers in human and mouse, Nucleic Acids Res. 47 (D1) (2019) D721–d728.
[44] J. Ru, P. Li, J. Wang, et al., TCMSP: a database of systems pharmacology for drug discovery from herbal medicines, J. Cheminf. 6 (2014) 13.
[45] H.Y. Xu, Y.Q. Zhang, Z.M. Liu, et al., ETCM: an encyclopaedia of traditional Chinese medicine, Nucleic Acids Res. 47 (D1) (2019) D976–d982.
[46] X. Xue, X. Zhao, J. Wang, et al., Carthami flos extract against carbon tetrachloride-induced liver fibrosis via alleviating angiogenesis in mice, Phytomedicine 108 (2023) 154517.
[47] Y. Wang, Z. Wang, C. Wang, et al., [Mechanism of Carthami Flos and Lepidii Semen drug pair in inhibition of myocardial fibrosis by improving cardiac microenvironment based on network pharmacology and animal experiment], Zhongguo Zhongyao Zazhi 47 (3) (2022) 753–763.
[48] J. Wang, X. Li, H. Chang, et al., Network pharmacology and bioinformatics study on the treatment of renal fibrosis with persicae semen-carthami flos drug pair, Medicine (Baltim.) 102 (8) (2023) e32946.
[49] Q. Lu, W.Z. Zuo, X.J. Ji, et al., Ethanolic Ginkgo biloba leaf extract prevents renal fibrosis through Akt/mTOR signaling in diabetic nephropathy, Phytomedicine 22 (12) (2015) 1071–1078.
[50] S.Q. Liu, J.P. Yu, L. He, et al., [Effects of nuclear factor kappaB and transforming growth factor beta1 in the anti-liver fibrosis process using Ginkgo biloba extract], Zhonghua Gan Zang Bing Za Zhi 13 (12) (2005) 903–907.
[51] Y. Wang, R. Wang, Y. Wang, et al., Ginkgo biloba extract mitigates liver fibrosis and apoptosis by regulating p38 MAPK, NF-κB/IκBα, and Bcl-2/Bax signaling, Drug Des. Dev. Ther. 9 (2015) 6303–6317.
[52] X. Meng, D. Wang, H. Zhang, et al., Portulaca oleracea L. extract relieve mice liver fibrosis by inhibiting TLR-4/NF-κB, Bcl-2/Bax and TGF-β1/Smad2 signalling transduction, Nat. Prod. Res. (2024) 1–9.
[53] H. Tian, L. Wang, T. Fu, Ephedrine alleviates bleomycin-induced pulmonary fibrosis by inhibiting epithelial-mesenchymal transition and restraining NF-κB signaling, J. Toxicol. Sci. 48 (10) (2023) 547–556.
[54] H.Q. Zhai, J.R. Hhang, M.C. Gao, et al., Comparative study between Ephedra sinica Stapf and Fructus Schisandrae Chinensis on ET-1 and 6-keto-prostaglandin F1α in rats with idiopathic pulmonary fibrosis, Genet. Mol. Res. 13 (2) (2014) 3761–3771.
[55] H.F. Lakatos, T.H. Thatcher, R.M. Kottmann, et al., The role of PPARs in lung fibrosis, PPAR Res. 2007 (2007) 71323.
[56] A.T. Reddy, S.P. Lakshmi, Y. Zhang, et al., Nitrated fatty acids reverse pulmonary fibrosis by dedifferentiating myofibroblasts and promoting collagen uptake by alveolar macrophages, Faseb. J. 28 (12) (2014) 5299–5310.
[57] J.E. Milam, V.G. Keshamouni, S.H. Phan, et al., PPAR-gamma agonists inhibit profibrotic phenotypes in human lung fibroblasts and bleomycin-induced pulmonary fibrosis, Am. J. Physiol. Lung Cell Mol. Physiol. 294 (5) (2008) L891–L901.
[58] K. Asada, S. Sasaki, T. Suda, et al., Antiinflammatory roles of peroxisome proliferator-activated receptor gamma in human alveolar macrophages, Am. J. Respir. Crit. Care Med. 169 (2) (2004) 195–200.
[59] Y.S. Yoon, S.Y. Kim, M.J. Kim, et al., PPARγ activation following apoptotic cell instillation promotes resolution of lung inflammation and fibrosis via regulation of efferocytosis and proresolving cytokines, Mucosal Immunol. 8 (5) (2015) 1031–1046.
[60] A. Chawla, W.A. Boisvert, C.H. Lee, et al., A PPAR gamma-LXR-ABCA1 pathway in macrophages is involved in cholesterol efflux and atherogenesis, Mol. Cell 7 (1) (2001) 161–171.
[61] C. Schneider, S.P. Nobs, M. Kurrer, et al., Induction of the nuclear receptor PPAR-γ by the cytokine GM-CSF is critical for the differentiation of fetal monocytes into alveolar macrophages, Nat. Immunol. 15 (11) (2014) 1026–1037.
[62] T. Tsukui, S. Ueha, J. Abe, et al., Qualitative rather than quantitative changes are hallmarks of fibroblasts in bleomycin-induced pulmonary fibrosis, Am. J. Pathol. 183 (3) (2013) 758–773.
[63] J. Hou, J. Ji, X. Chen, et al., Alveolar epithelial cell-derived Sonic hedgehog promotes pulmonary fibrosis through OPN-dependent alternative macrophage activation, FEBS J. 288 (11) (2021) 3530–3546.
[64] A.S. Neupane, M. Willson, A.K. Chojnacki, et al., Patrolling alveolar macrophages conceal bacteria from the immune system to maintain homeostasis, Cell 183 (1) (2020) 110–125.e11.
[65] A. Nakamura, R. Ebina-Shibuya, A. Itoh-Nakadai, et al., Transcription repressor Bach2 is required for pulmonary surfactant homeostasis and alveolar macrophage function, J. Exp. Med. 210 (11) (2013) 2191–2204.
[66] P. Popovics, K.O. Skalitzky, E. Schroeder, et al., Steroid hormone imbalance drives macrophage infiltration and Spp1/osteopontin(+) foam cell differentiation in the prostate, J. Pathol. 260 (2) (2023) 177–189.
[67] Z. Liu, Z. Gao, B. Li, et al., Lipid-associated macrophages in the tumor-adipose microenvironment facilitate breast cancer progression, OncoImmunology 11 (1) (2022) 2085432.
[68] Y. Dong, A.A. Arif, J. Guo, et al., CD44 loss disrupts lung lipid surfactant homeostasis and exacerbates oxidized lipid-induced lung inflammation, Front. Immunol. 11 (2020) 29.
[69] M. Plataki, A.V. Koutsopoulos, K. Darivianaki, et al., Expression of apoptotic and antiapoptotic markers in epithelial cells in idiopathic pulmonary fibrosis, Chest 127 (1) (2005) 266–274.
[70] S.K. Natarajan, T. Bruett, P.G. Muthuraj, et al., Saturated free fatty acids induce placental trophoblast lipoapoptosis, PLoS One 16 (4) (2021) e0249907.